Quasi-periodic structure of Landau magnetic levels and absorption spectra of GaAs - (Ga,Al)As Fibonacci superlattices under in-plane magnetic fields

1997 J. Phys.: Condens. Matter 9 1005

(http://iopscience.iop.org/0953-8984/9/5/007)

J. Phys.: Condens. Matter **9** (1997) 1005–1017. Printed in the UK PII: S0953-8984(97)75587-5

Quasi-periodic structure of Landau magnetic levels and absorption spectra of GaAs–(Ga,Al)As Fibonacci superlattices under in-plane magnetic fields

M de Dios-Leyva†, A Bruno-Alfonso† and Luiz E Oliveira‡

† Department of Theoretical Physics, University of Havana, San Lázaro y L, Vedado 10400, Havana, Cuba

‡ Instituto de Física, Universidade Estadual de Campinas, CP6165, Campinas, São Paulo 13083-970, Brazil

Received 18 June 1996, in final form 14 October 1996

Abstract. A detailed theoretical study, in the effective-mass approximation, of the magnetic Landau subbands, wavefunctions, and intraband and interband absorption coefficients of quasi-periodic GaAs–(Ga,Al)As Fibonacci superlattices under in-plane magnetic fields is presented. Calculations are performed for in-plane magnetic fields related by τ^2 and τ^4, with $\tau = (1 + 5^{1/2})/2$ being the golden mean, and for magnetic fields appropriate for comparison with experimental measurements. It is shown that, for a given sample and in-plane magnetic field, the Landau magnetic subbands exhibit a Fibonacci-like quasi-periodic structure, and that these quasi-periodic properties are extremely useful in avoiding integration over the full range of cyclotron orbit centre positions. The intraband absorption spectra are calculated, at a given temperature, for n-doped GaAs–(Ga,Al)As Fibonacci superlattices under in-plane magnetic fields scaled by τ^{2n}, and the theoretical absorption spectra are shown to be self-similar (for even n) and anti-self-similar (for odd n). For the interband magneto-absorption spectra of GaAs–(Ga,Al)As Fibonacci superlattices, we find a self-similar behaviour of the interband absorption spectra for magnetic fields scaled by τ^{2n}, in agreement with available experimental data. The interband absorption coefficients are also evaluated for various in-plane magnetic fields with good overall agreement with experimental measurements.

1. Introduction

The discovery of quasi-crystals [1], i.e. solids intermediate between completely periodic crystals and random or disordered amorphous solids, has stimulated the study of the physical properties of one-dimensional quasi-periodic superlattices. Further stimulus for such a study arises as modern growth techniques such as molecular beam epitaxy (MBE) and metal–organic chemical vapour deposition (MOCVD) have made possible the realization of high-quality semiconducting-heterostructure systems consisting of alternating layers of different semiconductors with controlled layer thicknesses and sharp interfaces between them. The first realization of such a quasi-periodic superlattice was reported by Merlin *et al* [2] and consisted of MBE-grown alternating layers of GaAs and AlAs, forming a Fibonacci sequence in which the ratio of incommensurate periods was approximately equal to the golden mean $\tau = (1 + 5^{1/2})/2$. Since this progress was made, there has been an increasing interest in the study of the physical properties of Fibonacci superlattices (FSLs). This is because such a system presents self-similarity and constitute a simple and typical example of quasi-periodic systems.

0953-8984/97/051005+13$19.50

In the past few years, the optical properties of FSLs have been the subject of intensive theoretical and experimental studies. Spectroscopic ellipsometry, photoluminescence excitation spectroscopy, picosecond luminescence measurements and reflectance spectroscopy have been used to study the optical properties of GaAs–(Ga,Al)As FSLs. Garriga *et al* [3] reported the ellipsometry spectra of a GaAs– AlAs FSL, a GaAs–AlAs Thue–Morse SL and a GaAs–AlAs random-sequence SL and compared the experimental results with calculations of a model dielectric function within a Kronig–Penney-like potential, suggesting a correspondence between the steps in the theoretical lineshapes and the observed peaks. Laruelle and Etienne [4] performed photoluminescence excitation (PLE) spectroscopy measurements of two types of GaAs–(Ga,Al)As FSL, recalled the importance of the energy dependence of the Fibonacci invariant [5] in characterizing the band structure, wavefunction localization and how both are related and compared the position of the observed structures with the calculated values of the transition energies using the envelope-function approximation. Yamaguchi *et al* [6] investigated the electronic structure and the perpendicular transport properties of photoexcited carriers in a GaAs–AlAs FSL with an enlarged well by means of PLE and picosecond luminescence measurements. They argued that the degree of localization in the Fibonacci system was intermediate between those of a periodic and random SLs and found the observed PLE spectra to be in good agreement with the calculated density of states (corresponding to the conduction band carriers), obtained by using a transfer-matrix technique in the envelope-function approximation, for the Fibonacci, random and periodic systems. Photocurrent spectroscopy under an electric field applied along the growth axis was used by Laruelle *et al* [7] to investigate the wavefunction localization in a quasi-periodic GaAs–$Ga_{0.75}Al_{0.25}As$ FSL, and they explain the effects of the electric field on the photocurrent spectra via a simple tight-binding analysis based on knowledge of the electronic structure at zero field. More recently, Munzar *et al* [8] have measured the normal-incidence reflectance for GaAs–(Ga,Al)As FSLs in the temperature range from 20 to 300 K and developed a simple theoretical model to calculate the reflectance with the energy levels calculated with the help of the envelope-function approximation and the Kohmoto–Kadanoff–Tang [9] renormalization group method. Their calculations reveal the multifractal properties of the electron energy spectrum and the self-similarity of the wavefunction of the ground state. Also, they found the model predictions to be in good agreement with experiment and showed that the multifractal properties of the electronic structure of FSLs manifest themselves also in the experimental reflectance spectra.

The effects of a magnetic field parallel to the layers ($B_{\|}$ configuration) in a GaAs–(Ga,Al)As FSL where theoretically investigated by Wang and Maan [10] who showed that self-similarity on the length scale is reproduced in the energy-level structure, and that the fractal property is a consequence of the identical behaviour of the Hamiltonian and the Fibonacci potential. In particular, they have demonstrated that the cyclotron-orbit-centre dispersion of the energy levels shows a field-dependent structure which is self-similar or anti-self-similar for fields related to integer powers of the τ golden mean. Experimentally, the existence of Landau levels in GaAs–(Ga,Al)As FSLs with magnetic fields applied parallel to the layers was clearly observed by Toet *et al* [11]. Moreover, they measured the magneto-optical absorption spectra of this system and suggested that the spectra exhibit self-similarity at magnetic-field values scaled by τ. Bruno-Alfonso *et al* [12, 13] have recently calculated the magnetic subbands and electron wavefunctions, by using an expansion in harmonic-oscillator wavefunctions, and showed that the intraband and interband transition strengths exhibit self-similarity or anti-self-similarity at different magnetic-field values (related by integer powers of τ). They have also shown that the corresponding absorption spectra essentially exhibit a self-similar or an anti-self-similar

behaviour, with the width of the interband peaks increasing linearly with increasing field in agreement with the experimental results obtained by Toet *et al* [11]. The above theoretical and experimental results on the optical properties of FSLs in the $B_{\parallel}$ configuration have motivated us to perform theoretically a systematic study of the GaAs–(Ga,Al)As FSLs in such a configuration in order to understand the quasi-periodic and fractal-structure properties of the systems better.

The paper is organized as follows. Section 2 contains a description of the theoretical framework and the method of calculation of the electron and hole energy levels, wavefunctions and absorption spectra of a GaAs–(GaAl)As FSL under in-plane magnetic fields. A detailed presentation of the calculated results, a comparison with the measured interband absorption measurements, and discussion is given in section 3. Finally, in section 4 we present our conclusions.

2. Theory

We consider a GaAs–(Ga,Al)As FSL with growth axis in the y direction and under an applied magnetic field and work within the effective-mass approximation. By considering the parabolic band scheme to model both electron and hole levels, the effective Hamiltonian for carriers in both the conduction and the valence subbands is

$$H = \frac{1}{2m_\alpha^*}\left(\boldsymbol{p} + \frac{e\boldsymbol{A}}{c}\right)^2 + V_\alpha(y) \tag{2.1}$$

where m_α^* are the conduction or valence effective masses, e is the proton charge, $\boldsymbol{p}$ is the momentum operator, $\boldsymbol{A}$ is the vector potential, α refers to either the conduction (c) or the valence (v) subbands, and $V_\alpha(y)$ is the FSL potential, defined below. We consider the dielectric constant and effective masses to be constant across the interfaces and choose barrier potentials for electrons and holes following the usual 60%–40% rule with respect to the ΔE_g band-gap difference between GaAs and $Ga_{1-x}Al_xAs$, with $\Delta E_g(\mathrm{eV}) = 1.247x$. The magnetic field is taken as parallel to the interfaces, $\boldsymbol{B} = (0, 0, B)$, and the gauge for the vector potential is chosen as $\boldsymbol{A} = (-yB, 0, 0)$. As the Hamiltonian is translational invariant in the x and z directions, the wavefunctions may be taken as

$$|n_\alpha, k_x, k_z\rangle = \frac{\exp(\mathrm{i}k_x x)}{L_x^{1/2}}\frac{\exp(\mathrm{i}k_z z)}{L_z^{1/2}}\Psi_{n_\alpha,k_x}(y) \tag{2.2}$$

where n_α are the Landau indices and L_x and L_z are the linear dimensions of the sample in the x and z directions, respectively.

$\Psi_{n_\alpha,k_x}(y)$ in equation (2.2) satisfies the following one-dimensional Schrödinger equation:

$$\left[\frac{p_y^2}{2m_\alpha^*} + \tfrac{1}{2}m_\alpha^*\omega_\alpha^2(y - y_0)^2 + \frac{\hbar^2k_z^2}{2m_\alpha^*} + V_\alpha(y)\right]\Psi_{n_\alpha,k_x}(y) = E_{n_\alpha}(k_x, k_z)\Psi_{n_\alpha,k_x}(y) \tag{2.3}$$

where $\omega_\alpha = eB/cm_\alpha^*$ is the cyclotron frequency, $y_0 = k_x l_B^2$ is the cyclotron orbit centre position, $l_B = (\hbar c/eB)^{1/2}$ is the cyclotron radius,

$$E_{n_\alpha}(k_x, k_z) = \varepsilon_{n_\alpha}(k_x) + \frac{\hbar^2k_z^2}{2m_\alpha^*} \tag{2.4}$$

is the carrier energy corresponding to the full Hamiltonian (2.1) and $\varepsilon_{n_\alpha}(k_x)$ corresponds to the Landau magnetic levels for $k_z = 0$. Energies are measured with origin at the bottom (top) of the conduction (valence) band of the GaAs bulk (E_g), and with convenient orientations

for electrons and holes. Equation (2.3) is solved via an expansion of $\Psi_{n_\alpha,k_x}(y)$ in terms of harmonic-oscillator functions.

The magneto-optical absorption coefficient is proportional to the transition probability per unit of time involving initial and final states $|i\rangle$ and $|f\rangle$, respectively, and may be obtained via the Fermi golden rule:

$$W(\omega) = \frac{2\pi}{\overline{h}} \sum_{i,f} |\langle f|H_{int}|i\rangle|^2 \delta(E_f - E_i - \overline{h}\omega)[f(E_i) - f(E_f)] \tag{2.5}$$

where $H_{int} = (eA/m_0c)\varepsilon \cdot (\boldsymbol{p} + e\boldsymbol{A}/c)$ corresponds to the electron–photon interaction, ε is the polarization vector in the direction of the radiation electric field, m_0 is the free-electron mass, $\overline{h}\omega$ is the photon energy and $f(E)$ is the Fermi–Dirac occupation number.

In the effective-mass approximation, the magneto-optical $\alpha(\omega)$ absorption coefficient for a GaAs–(Ga,Al)As FSL is therefore given by

$$\alpha(\omega) = \frac{8\pi^2 e^2}{m_0^2 c\eta V\omega} \sum_{i,f} \left| \left\langle f \left| \varepsilon \cdot \left(\boldsymbol{p} + \frac{e\boldsymbol{A}}{c} \right) \right| i \right\rangle \right|^2 \delta(E_f - E_i - \overline{h}\omega)[f(E_i) - f(E_f)] \tag{2.6}$$

where $V = L_x L_z L_n$, η is the refraction index (taken as equal to 3.5) and L_n is the length of the ω_n FSL generation. In the above equation, we replace δ function by a broadened Lorentzian in order to model scattering resolution effects. At the temperature $T = 0$, it is straightforward to obtain the FSL *interband* magneto-optical $\alpha(\omega)$ absorption coefficient

$$\alpha(\omega) = \frac{2e^2(\varepsilon \cdot \boldsymbol{p}_{cv})^2}{m_0^2 c\eta l_B^2 \omega} \sum_{n_c,n_v} \frac{1}{\xi_n} \int_0^{\xi_n} \mathrm{d}\xi_0 \, |\langle \Psi_{n_c,\xi_0}(y)|\Psi_{n_v,\xi_0}(y)\rangle|^2 H_{n_c,n_v}(\xi_0,\omega) \tag{2.7}$$

with

$$H_{n_c,n_v}(\xi_0,\omega) = \int_{-\infty}^{\infty} \frac{\gamma \,\mathrm{d}x}{[x^2 - E_{n_c,n_v}(\xi_0,\omega)]^2 + \gamma^2} \tag{2.8}$$

$$E_{n_c,n_v}(\xi_0,\omega) = \overline{h}\omega - [E_g + \varepsilon_{n_c}(\xi_0) + \varepsilon_{n_v}(\xi_0)] \tag{2.9}$$

where $\boldsymbol{p}_{cv}$ is the momentum matrix element between the conduction and valence Bloch functions at the Γ point, γ is half the energy broadening parameter, ξ_0 is the cyclotron y_0 orbit centre position in units of l_B, and ξ_n is L_n/l_B.

In the case of intraband transitions, our calculations will be performed in the $B_\parallel$ configuration with light propagation perpendicular to the magnetic field (Voigt geometry); we choose the polarization vector ε of the radiation as parallel to the x axis. One should note that intraband absorption properties may be experimentally studied by performing experiments on the magnetoabsorption in n-doped GaAs–(Ga,Al)As FSLs. Of course, such an experiment [14] should be carried out for low doping levels and a sufficiently high temperature in order to ensure that most of the donor electrons are in the magnetic conduction subbands. The (conduction) *intraband* magneto-optical $\alpha(\omega)$ absorption coefficient for GaAs–(Ga,Al)As FSL, at the temperature T, may be obtained by using a Maxwell–Boltzmann distribution for the carriers in the Landau magnetic subbands and is given as

$$\alpha(\omega) = \frac{2\pi^2 N e^2 \overline{h}\omega_c}{\eta c m_c^* \omega} \sum_{n_c',n_c} \int_0^{\xi_n} \mathrm{d}\xi_0 \, T_{n_c,n_c'}(\xi_0)[N_{n_c}(\xi_0) - N_{n_c'}(\xi_0)]\delta[\varepsilon_{n_c'}(\xi_0) - \varepsilon_{n_c}(\xi_0) - \overline{h}\omega] \tag{2.10}$$

with

$$T_{n_c,n_c'}(\xi_0) = |\sqrt{2}\langle \Psi_{n_c',\xi_0}(\xi)|(\xi - \xi_0)|\Psi_{n_c,\xi_0}(\xi)\rangle|^2 \tag{2.11}$$

$$N_{n_c}(\xi_0) = \frac{\exp[-\beta\varepsilon_{n_c}(\xi_0)]}{h(\xi_n)} \tag{2.12}$$

and

$$h(\xi_n) = \sum_{n_c} \int_0^{\xi_n} \mathrm{d}\xi_0 \, \exp[-\beta\varepsilon_{n_c}(\xi_0)]. \tag{2.13}$$

In the above intraband equations, $\beta = 1/k_B T$ and N is the number of donor electrons per unit of volume at the conduction subband which was taken as 10^{15} cm^{-3}.

The results presented in this work for the magneto-absorption interband and intraband spectra of GaAs–(Ga,Al)As FSLs were obtained using the above expressions and convergence was achieved with 500, 400 and 300 harmonic-oscillator wavefunctions (or Landau levels) in the basis set for B/τ^4, B/τ^2 and B, respectively. Also, we have made a periodic approximation for the FSL potential corresponding to a given ω_n generation (see discussion below) and considered a periodic SL whose unit cell is based on the ω_n FSL potential. Of course, this periodic approach is physically sound when n is large enough.

3. Results and discussion

We now focus on the ω_{13} generation of a GaAs–(Ga,Al)As FSL studied by Wang and Maan [10], Toet *et al* [11] and Bruno-Alfonso *et al* [12, 13]. The heterostructure consists of a FSL sequence of alternating layers of elementary blocks a and b, consisting of potential barriers of $Ga_{1-x}Al_xAs$ and wells of GaAs, respectively. A generation ω_n of the GaAs–(Ga,Al)As FSL may be obtained by taking $\omega_1 = a$ and $\omega_2 = b$ and using the recurrence relations $\omega_n = \omega_{n-2}\omega_{n-1}$ if n is odd, and $\omega_n = \omega_{n-1}\omega_{n-2}$ for n even. Notice that the inversion of the concatenation order at each generation is, in principle, not necessary to obtain a Fibonacci superlattice; the above choice of defining the FSL is motivated by the experimental construction [11] of the FSL (the self-similarity and anti-self-similarity discussed below is also obtained when the other definition [7] is used). By defining $F_1 = F_2 = 1$ and taking the Fibonacci sequence $F_n = F_{n-1} + F_{n-2}$, one has F_n, F_{n-2} and F_{n-1} for the total number of elementary blocks and for the number of elementary blocks $\underline{a}$ and $\underline{b}$, respectively, in the ω_n generation of the GaAs–(Ga,Al)As FSL, with the ratio F_n/F_{n-1} converging towards the τ golden mean value for large n. The above generation procedure described results in the self-similarity of the following structures: ω_n goes into ω_{n-2} under the transformations $ab \to a$ and $abb \to b$ whereas ω_n goes into the $\underline{\omega}_{n-1}$ reverse of ω_{n-1} by transforming $b \to a$ and $ab \to b$. It also follows [15] that, if one defines 'words' $W_a^k = \omega_k$ and $W_b^k = \omega_{k+1}$, then the Fibonacci sequence at the nth generation may be considered as being composed of words W_a^k and W_b^k arranged in a generation ω_{n+1-k}, for odd k, or the reverse of ω_{n+1-k} for even k, i.e. $\omega_n = \omega_{n+1-k}(W_a^k = \omega_k;\ W_b^k = \omega_{k+1})$, for odd k, and $\omega_n = \underline{\omega}_{n+1-k}(W_a^k = \omega_k;\ W_b^k = \omega_{k+1})$, for even k.

Theoretical calculations are performed for the ω_{13} generation of a GaAs–(Ga,Al)As FSL with parameters appropriate for comparison with the work by Wang and Maan [10] and Toet *et al* [11]. The values [4] of the valence and conduction effective masses are taken as $m_v^* = 0.34m_0$ and $m_c^* = 0.067m_0$, respectively. Also, the Al concentration $x = 0.2$, and the widths of the elementary barriers and wells are chosen as $d_a = 1.12$ nm and $d_b = 1.69$ nm, respectively, so that $d_a/d_b \simeq \tau$, and self-similarity or anti-self-similarity on the length scale for magnetic fields related by τ^{2n} is guaranteed [10–13] (for that purpose, we have performed calculations with $B = 20$ T, $B/\tau^2 = 7.64$ T and $B/\tau^4 = 2.92$ T).

The Landau conduction levels for the ω_{13} generation of a GaAs–$Ga_{0.8}Al_{0.2}As$ FSL are shown in figure 1 as functions of the y_0 cyclotron orbit centre, and for magnetic fields related by τ^2 and τ^4. In order to understand properly the properties of the Landau-energy spectra, it is convenient to consider the construction of the ω_{13} generation in

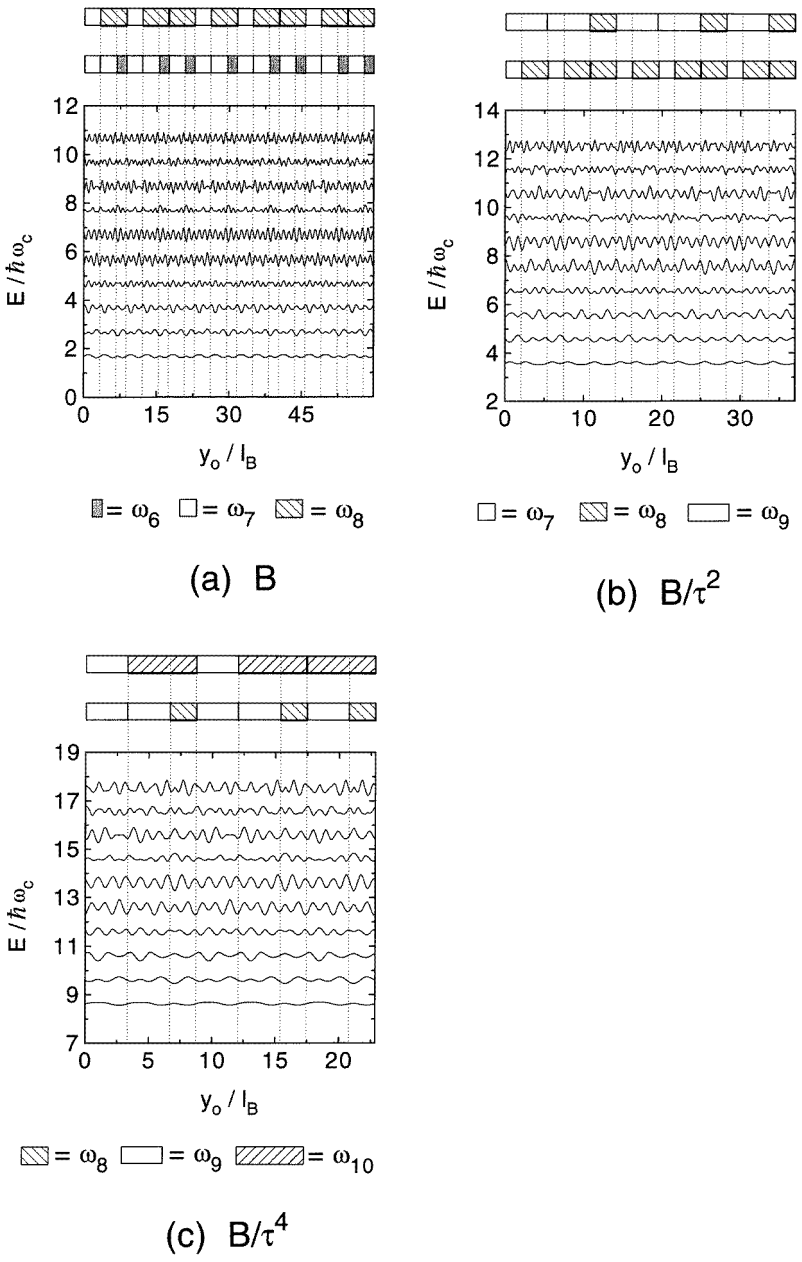

Figure 1. Landau conduction magnetic levels in reduced units, for the ω_{13} generation of a GaAs–$Ga_{0.8}Al_{0.2}As$ FSL, as functions of the reduced cyclotron orbit centre measured from an origin on the left side of the ω_{13} Fibonacci generation. The ω_{13} generation is pictorially shown twice in the upper part of the figure in terms of blocks of ω_k and ω_{k+1} generations, depicted at the bottom. Results are shown for the ten lowest Landau subbands, and for in-plane magnetic fields (*a*) $B = 20$ T, (*b*) $B/\tau^2 = 7.64$ T, and (*c*) $B/\tau^4 = 2.92$ T.

terms of blocks of 'words', as commented on before. For example, the ω_{13} generation may be obtained from blocks ω_7 and ω_8, and therefore, as depicted at the top of

Table 1. Length L_n of the W_n generation of a GaAs–(Ga,Al)As FSL up to $n = 13$; also shown are the magnetic length (or cyclotron radius) l_B for magnetic fields $B = 20$ T, $B/\tau^2 = 7.64$ T and $B/\tau^4 = 2.92$ T.

n	L_n (nm)	n	L_n (nm)	B (T)	L_B (nm)
1	1.12	8	30.93	20	5.74
2	1.69	9	50.05	7.64	9.28
3	2.81	10	80.98	2.92	15.01
4	4.50	11	131.03		
5	7.31	12	212.01		
6	11.81	13	343.04		
7	19.12				

Table 2. Localization length $R_n = 2.25[(2n + 1)/2]^{1/2} l_B$ of the magnetic Landau levels associated with the nth subband, for $B = 20$ T.

n	R_n (nm)	n	R_n (nm)
0	9.13	5	30.29
1	15.82	6	32.93
2	20.42	7	35.37
3	24.17	8	37.66
4	27.40	9	39.81

figure 1(a), $\omega_{13} = \omega_7(W_a^k = \omega_7; W_b^k = \omega_8) = \omega_7\omega_8\omega_7\omega_8\omega_8\omega_7\omega_8\omega_7\omega_8\omega_8\omega_7\omega_8\omega_8$. For other constructions of ω_{13} in terms of ω_6 and ω_7, ω_8 and ω_9, and ω_9 and ω_{10}, see top of figures 1(a), 1(b) and 1(c), respectively. It is clear from figure 1(a) that the six lowest ($n = 0, 1, 2, 3, 4, 5$) Landau subbands exhibit a $\underline{\omega}_8$ *Fibonacci-like quasi-periodic structure*, which corresponds to a decomposition of $\underline{\omega}_{13}$ in terms of 'words' ω_6 and ω_7, i.e. $\omega_{13} = \underline{\omega}_8$ ($W_a^k = \omega_6$; $W_b^k = \omega_7$), whereas the Landau subbands $n = 6, 7, 8, 9$ show a ω_7 *Fibonacci-like quasi-periodic structure*, associated with $\omega_{13} = \omega_7$ ($W_a^k = \omega_7$; $W_b^k = \omega_8$). Of course, the scaled FSL potentials seen by the electrons depend on the applied magnetic fields, and therefore the Landau-subband quasi-periodic structure may be understood by comparing in tables 1 and 2 the various physical lengths involved in the problem. Note in figure 1(a) that the 'words' ω_7 and ω_6 essentially appear with two 'neighbours' ω_6 and ω_7 in both sides, and therefore Landau levels corresponding to $n = 0, 1, 2, 3, 4, 5$, with localization lengths (see table 2) less than the sum of the lengths of ω_6 and ω_7 (equal to 30.93 nm; see table 1) exhibit a $\underline{\omega}_8$ Fibonacci-like quasi-periodic structure (as electrons corresponding to these Landau levels, and with equivalent orbit centre positions, essentially 'see' the same neighbourhood, i.e. the same scaled FSL potential), whereas Landau levels associated with $n = 6, 7, 8, 9$ with localization lengths less than the sum of the lengths of ω_7 and ω_8 (equal to 50.05 nm; see table 1) show a ω_7 Fibonacci-like quasi-periodic structure. One may similarly understand the quasi-periodic behaviour of the Landau levels in figures 1(b) and 1(c). The above behaviour follows from the self-similarity and scaling properties of the FSL which can be described not only as a sequence ω_n of blocks a and b, but also as a Fibonacci sequence of two arbitrary consecutive generations ω_k and ω_{k+1}. To our knowledge, this is the first time that this Landau-subband Fibonacci-like quasi-periodic structure has been pointed out in FSLs. Of course, depending on the strength of the in-plane magnetic field and on the Landau index of the magnetic subband, complete knowledge of a Landau magnetic subband would require only the calculation in two specific 'words'

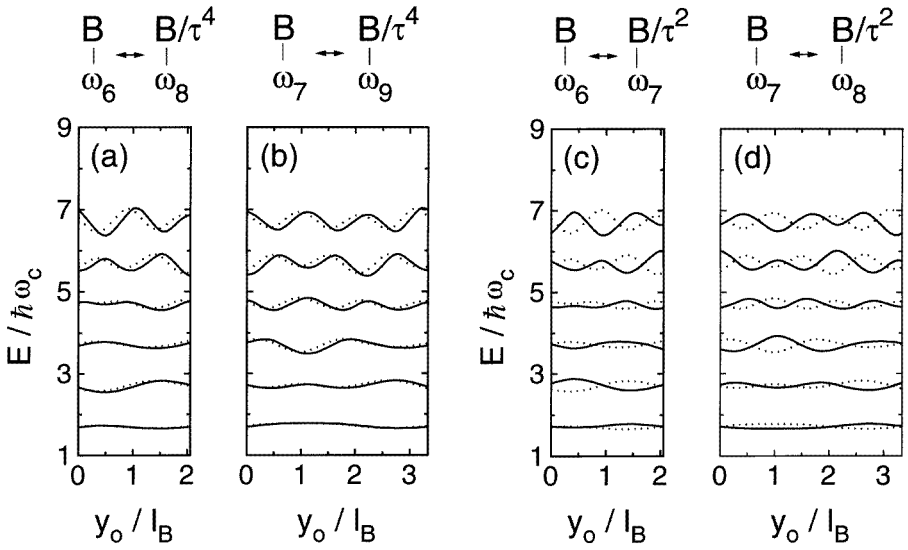

Figure 2. Landau conduction magnetic levels (in units of the cyclotron energy) of a GaAs–$Ga_{0.8}Al_{0.2}As$ FSL as functions of the reduced cyclotron orbit centre measured from an origin on the left side of each ω_n Fibonacci generation. Magnetic levels are shown for the six lowest Landau subbands, and for the values of in-plane magnetic fields $B = 20$ T, $B/\tau^2 = 7.64$ T and $B/\tau^4 = 2.92$ T. Results are shown for Fibonacci blocks (*a*) ω_6 (for B) ω_8 (for B/τ^4) generations, (*b*) ω_7 (for B) and ω_9 (for B/τ^4), (*c*) ω_6 (for B) and ω_7 (for B/τ^2) and (*d*) ω_7 (for B) and ω_8 (for B/τ^2).

ω_k and ω_{k+1} corresponding to a ω_{n+1-k} Fibonacci-like quasi-periodic structure. Figure 2 therefore presents all the information concerned with the six lowest conduction magnetic Landau subbands for magnetic fields scaling with τ^2 and τ^4, i.e. in 'words' ω_6 and ω_7 for $B = 20$ T, 'words' ω_7 and ω_8 for $B/\tau^2 = 7.64$ T, and ω_8 and ω_9 for $B/\tau^4 = 2.92$ T. Notice the similarity (for $B = 20$ T and $B/\tau^4 = 2.92$ T) and anti-self-similarity (for $B = 20$ T and $B/\tau^2 = 7.64$ T) of the energy levels; of course, as the reduced cyclotron orbit centre is measured from an origin on the left side of each ω_n Fibonacci generation, the similarity properties would hold if one considers a small horizontal shift of the origin of one of the cyclotron orbit centres (notice that, if one removes the first and last elementary blocks of a given generation ω_n, one obtains a modified Fibonacci generation which contains an inversion centre [16]; in that case, by considering the origin of the cyclotron orbit centres at the inversion centre, the similarity properties would directly appear [13], with no shift needed, for sufficiently large n).

Figure 3 presents the wavefunctions of the Landau conduction ground and first excited states plotted along the growth direction of the FSL, for an in-plane magnetic field of $B/\tau^4 = 2.92$ T, and for six different and equivalent cyclotron orbit centres, corresponding to the beginning of the ω_9 generation. Electrons corresponding to these orbit centre positions essentially 'see' the same FSL potential and present self-similar wavefunctions. It is clear, therefore, from figure 1(*c*) and figure 3 that the $n = 0$ and 1 Landau subbands and electron wavefunctions exhibit, for a magnetic field of $B/\tau^4 = 2.92$ T, a $\underline{\omega_6}$ *Fibonacci-like quasi-periodic structure*, as functions of the orbit centre position. Of course, it is straightforward to see that this result is quite general and applies to different in-plane magnetic fields and magnetic subbands, resulting in other quasi-periodic structures.

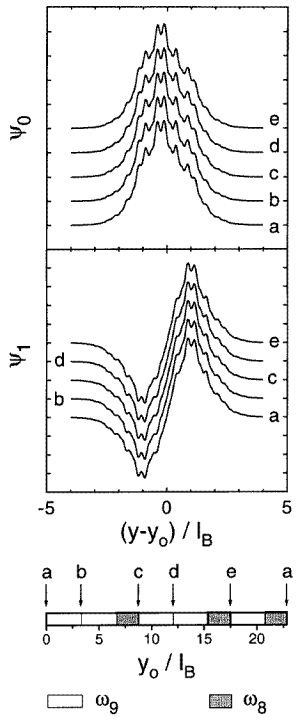

Figure 3. Ground-state $n = 0$ and first-excited-state $n = 1$ Landau conduction wavefunctions Ψ_n ($x = z = 0$, y) of a GaAs–$Ga_{0.8}Al_{0.2}As$ FSL, associated with cyclotron orbit centres y_0 at positions a, b, c, d and e in the ω_{13} Fibonacci generation, pictorially shown at the bottom part of the figure in terms of blocks of ω_8 and ω_9 generations. Results are shown for an in-plane magnetic field $B/\tau^4 = 2.92$ T. The wavefunctions have been offset vertically for clarity.

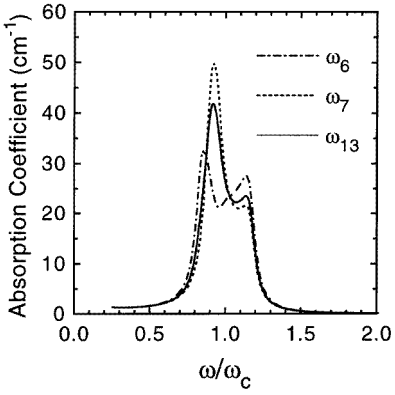

Figure 4. Intraband absorption coefficient $\alpha(\omega)$ for the ω_{13} generation of n-doped (10^{15} cm^{-3}) GaAs–$Ga_{0.8}Al_{0.2}As$ FSL (——), obtained by weighting the partial contributions obtained from blocks of ω_6 generation (— · —) and ω_7 generation (- - - -). Results are shown for $T = 70$ K and an in-plane magnetic field of 20 T.

Owing to the above-mentioned properties, it is clear that the intraband absorption coefficient $\alpha(\omega)$ for the ω_{13} generation of an n-doped [14] (10^{15} cm^{-3}) GaAs–$Ga_{0.8}Al_{0.2}As$ FSL may be obtained by an appropriate weighting of the partial contributions from blocks of ω_6 and ω_7 generations, and this is depicted in figure 4, for $T = 70$ K and for an in-plane magnetic field of 20 T, and for a Γ energy broadening parameter of 3 meV in a Lorentzian representation of the δ function in equation (2.10). Of course, a similar procedure may be performed for the interband coefficient in terms of the ω_6 and ω_7 generations, and it is clear, therefore, that the quasi-periodic properties are extremely useful in avoiding integration over the full range of cyclotron orbit centre positions [17]. A comparison between the scaled intraband absorption coefficient $\alpha(\omega)$ associated with in-plane magnetic fields scaled by τ^4 and τ^2 is presented in figure 5. Results are shown for $T = 70$ K and a Γ broadening parameter of 3 meV in the case of $B = 20$ T, with corresponding scalings of τ^4 and τ^2 for $B = 2.92$ T and 7.64 T, respectively. The self-similarity of the intraband absorption coefficient for $B = 20$ T and $B/\tau^4 = 2.92$ T, and the anti-self-similarity for $\alpha(\omega)$ in the case of $B = 20$ T and $B/\tau^2 = 7.64$ T are clearly seen in figure 5.

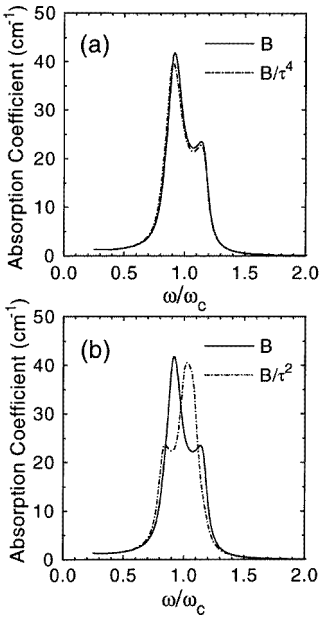

Figure 5. Intraband absorption coefficient $\alpha(\omega)$ for the ω_{13} generation of an n-doped GaAs–$Ga_{0.8}Al_{0.2}As$ FSL. Results are shown for in- plane magnetic fields (*a*) $B = 20$ T (——) and $B/\tau^4 = 2.92$ T (— · —) and (*b*) $B = 20$ T (——) and $B/\tau^2 = 7.64$ T (— · —) and for $T = 70$ K and temperatures scaled by τ^4 and τ^2, respectively.

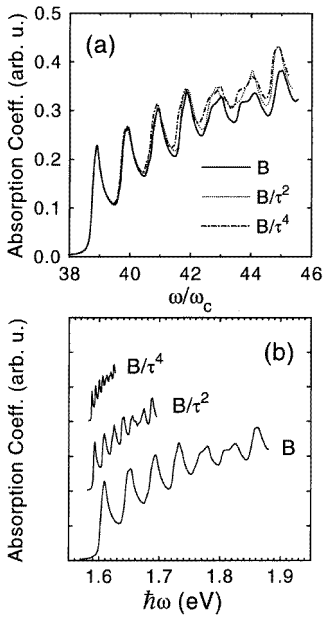

Figure 6. Interband absorption coefficient $\alpha(\omega)$ for the ω_{13} generation of a GaAs– $Ga_{0.8}Al_{0.2}As$ FSL. Results are shown for in-plane magnetic fields $B = 20$ T (——) $B/\tau^2 = 7.64$ T (· · · · ·) and $B/\tau^4 = 2.92$ T (— · —). Results are in reduced units of energies in (*a*), whereas energies are in electronvolts in (*b*). The absorption coefficients in (*b*) have been offset vertically for clarity.

The interband absorption coefficients $\alpha(\omega)$ for the ω_{13} generation of a GaAs–$Ga_{0.8}Al_{0.2}As$ FSL are shown in figure 6, at $T = 0$ K, and for in-plane magnetic fields of $B = 20$ T, $B/\tau^2 = 7.64$ T and $B/\tau^4 = 2.92$ T. Results for $\alpha(\omega)$ in figure 6(*b*) are displayed with energies in electronvolts and obtained with scaled level broadenings of 4, $4/\tau^2$ and $4/\tau^4$ meV, respectively, whereas in figure 6(*a*) the interband absorption coefficients are appropriately scaled and energies are displayed in reduced units. Notice the self-similar behaviour of the interband absorption spectra for magnetic fields scaled by τ^{2n}, in agreement with the experimental results obtained by Toet *et al* [11]. Results for the interband absorption coefficients for various in-plane magnetic fields ($B = 10$, 14, 18 and 22 T) appropriate for comparison with the experimental results of Toet *et al* [11] are displayed in figure 7. In the specific calculation shown in figure 7, theoretical results were obtained with values of the valence and conduction effective masses taken as $m_v^* = [0.5m_0$ and $m_c^* = 0.074m_0$, respectively, and with an energy level broadening $\Gamma = 2$ meV in order to obtain the best fit with the experimental data [11]. As the excitonic part of the spectra is not shown in the experimental data of Toet *et al* [11], we have displayed the lines associated with transitions between ground-state valence and conduction magnetic Landau subbands as chain curves in figure 7. Of course, the conventional interpretation is that in principle all transitions are exciton like but weakly bound higher-energy transitions behave basically as free electron–hole transitions, whereas the ground-state transitions are strongly affected by excitonic effects, which are not taken into account in our theoretical

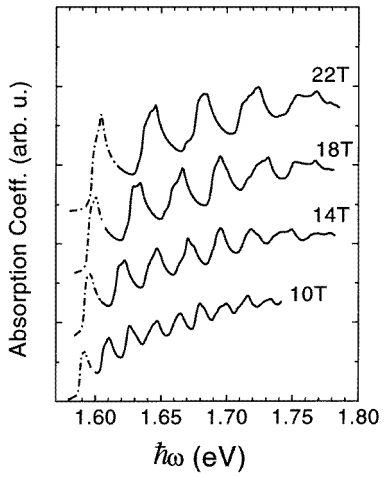

Figure 7. Interband absorption coefficient $\alpha(\omega)$ calculated for the ω_{13} generation of a GaAs–$Ga_{0.8}Al_{0.2}As$ FSL, and for various in-plane magnetic fields: — · —, curves associated with transitions between ground-state valence and conduction magnetic Landau subbands.

study. Also, we have not considered any valence band mixture and have modelled the valence band via a simple spherically averaged hole effective mass. It is important to notice, however, that one finds overall agreement between the experimental data and the theoretical calculations. The second peak in our theoretical calculations ($n_v = 1 \rightarrow n_c = 1$), for instance, shows a doublet structure (purely associated with valence and conduction subband dispersive effects), also apparent in the experimental data. Of course, complete quantitative understanding of the experimental measurements would require a theoretical treatment which should include valence band mixture, non-parabolicity, excitonic and scattering effects. Also, one must be aware that the validity of the similarity properties discussed in this section would break down for sufficiently high magnetic fields, high barriers, thick barriers and wells, and large values of the Landau subband index [10–13].

4. Conclusions

We have presented a detailed theoretical treatment, in the effective-mass approximation, of the magnetic Landau subbands, wavefunctions, and intraband and interband absorption coefficients of quasi-periodic GaAs–(Ga,Al)As FSLs under in-plane magnetic fields. Landau magnetic subbands and electron wavefunctions were obtained within a parabolic model for both the conduction and the valence bands, and through an expansion in harmonic-oscillator functions. Calculations were performed for in-plane magnetic fields related by τ^2 and τ^4, and for magnetic fields appropriate for comparison with experimental measurements. It is shown that, for a given sample and in-plane magnetic field, the Landau magnetic subbands exhibit a 'non-trivial' Fibonacci-like quasi-periodic structure. The specific ω_n Fibonacci quasi-periodicity associated with a given Landau magnetic subband depends on an interplay between the corresponding localization length of the states associated with the Landau subband and the length of the consecutive 'words' ω_k and ω_{k+1} used to describe the FSL. Also, we have demonstrated that, depending on the strength of the in-plane magnetic field and of the Landau index of the magnetic subband, complete knowledge of a Landau magnetic subband would require only the calculation in those two specific 'words'. Moreover, these quasi-periodic properties are extremely useful in avoiding integration over the full range

of cyclotron orbit centre positions and therefore enormously simplify the calculation of the magneto-absorption spectra. It is straightforward to see from the preceding discussion and equations (2.7) and (2.10) that the magneto-absorption coefficients are the same for different ω_n Fibonacci generations provided that n is large enough.

The intraband absorption spectra were calculated, at a given temperature, for n-doped (10^{15} cm^{-3}) GaAs–$Ga_{0.8}Al_{0.2}As$ FSLs under in-plane magnetic fields scaled by τ^{2n}, and the theoretical absorption spectra were shown to be self-similar (for even n) and anti-self-similar (for odd n). For the interband magneto-absorption spectra, at $T = 0$ K, of GaAs–$Ga_{0.8}Al_{0.2}As$ FSLs, one finds a self-similar behaviour of the interband absorption spectra for magnetic fields scaled by τ^{2n}, in agreement with the experimental results obtained by Toet *et al* [11]. The interband absorption coefficients were also evaluated for various in-plane magnetic fields and we found good overall agreement with the experimental results of Toet *et al* [11].

Acknowledgments

We are grateful to the hospitality of the International Centre of Theoretical Physics (Trieste, Italy) where part of this work was done. LEO is also grateful to the hospitality of the Department of Theoretical Physics of the University of Havana, where this work was completed, and to the Brazilian Agencies CNPq and FAEP-UNICAMP for partial financial support.

References

[1] Shechtman D, Blech I, Gratias D and Cahn J W 1984 *Phys. Rev. Lett.* **53** 1951
[2] Merlin R, Bajema K, Clarke R, Juang F Y and Bhattacharya P K 1985 *Phys. Rev. Lett.* **55** 1768
[3] Garriga M, Brey L, Nagle J and Ploog K 1988 *Proc. 19th Int. Conf. on the Physics of Semiconductors (Warsaw, 1988)* ed W Zawadzki (Warsaw: Polish Academy of Sciences) p 263
[4] Laruelle F and Etienne B 1988 *Phys. Rev.* B **37** 4816
[5] Kohmoto M and Oono Y 1984 *Phys. Lett.* **102A** 145
[6] Yamaguchi A A, Saiki T, Ninomiya T, Misawa K, Kobayachi T, Kuwata-Gonokami M and Yao T 1990 *Solid State Commun.* **75** 955
[7] Laruelle F, Paquet D, Joncour M C, Jusserand B, Barrau J, Mollot F and Etienne B 1990 *Springer Series in Solid-State Sciences* vol 97, ed F Kuchar, H Heinrich and G Bauer (Springer: Berlin) p 258
Laruelle R, Etienne B, Barrau J, Khirouni K, Brabant J C, Amand T and Brousseau M 1990 *Surf. Sci.* **228** 92
[8] Munzar D, Bocáek L, Humlícek J and Ploog K 1994 *J. Phys.: Condens. Matter* **6** 4107
[9] Kohmoto M, Kadanoff L and Tang C 1983 *Phys. Rev. Lett.* **50** 1870
[10] Wang Y Y and Maan J C 1989 *Phys. Rev.* B **40** 1955
[11] Toet D, Potemski M, Wang Y Y, Maan J C, Tapfer L and Ploog K 1991 *Phys. Rev. Lett.* **66** 2128
Toet D 1992 *Dokter Diss.* Universitat Konstanz
[12] Bruno-Alfonso A, Reyes-Gomez E, Oliveira L E and de Dios-Leyva M 1995 *J. Appl. Phys.* **78** 1379
[13] Bruno-Alfonso A, Oliveira L E and de Dios-Leyva M 1995 *Appl. Phys. Lett.* **67** 536
de Dios-Leyva M, Bruno-Alfonso A, Reyes-Gomez E and Oliveira L E 1995 *J. Phys.: Condens. Matter* **7** 9799
[14] Duffield T, Bhat R, Koza M, DeRosa F, Rush K M and Allen S J Jr 1987 *Phys. Rev. Lett.* **59** 2693
Duffield T, Bhat R, Koza M, Hwang D M, DeRosa F, Grabbe P and Allen S J Jr 1988 *Solid State Commun.* **65** 1483
[15] MacDonald A H 1987 *Interfaces, Quantum Wells, and Superlattices* ed C R Leavens and R Taylor (New York: Plenum) p 347
[16] Kölar M and Ali M K 1989 *Phys. Rev.* B **39** 426

[17] Small differences between the present results for the intraband and interband coefficients and previous [13] theoretical results may be traced back to essentially two reasons: first, no periodic conditions were imposed [13] in the ω_{13}-generation FSL potential and, second, in the previous calculation the range of cyclotron orbit centre positions used in the integration for $\alpha(\omega)$ was reduced in order to avoid 'end effects' in the actual calculation. Of course, the present calculation is more reliable.